



Removal of lead, cadmium, and mercury ions using biosorption

Abbas H. Sulaymon, Shahlaa E. Ebrahim*, Sama M. Abdullah, Tariq J. Al-Musawi

*Environmental Engineering Department, College of Engineering, Baghdad University, Baghdad, Iraq
Tel. 009647903971195; Email: shahlaaaga@yahoo.com*

Received 17 April 2010; accepted 21 November 2010

ABSTRACT

The biosorption of Pb (II), Cd (II), and Hg (II) from simulated aqueous solutions using baker's yeast biomass was investigated. Batch type experiments were carried out to find the equilibrium isotherm data for each component (single, binary, and ternary), and the adsorption rate constants. Kinetics pseudo-first and second-order rate models applied to the adsorption data to estimate the rate constant for each solute, the results showed that the Cd (II), Pb (II), and Hg (II) uptake process followed the pseudo-second-order rate model with (R^2) 0.963, 0.979, and 0.960, respectively. The equilibrium isotherm data were fitted with five theoretical models. Langmuir model provides the best fitting for the experimental results with (R^2) 0.992, 0.9987, and 0.9995 for Cd (II), Pb (II), and Hg (II), respectively. The effect of various influent adsorbates concentration, and flow rate on the performance of fixed bed adsorber was found for the three heavy metals. A mathematical model was formulated to describe the breakthrough curves in the fixed bed adsorber for each component. The results show that the mathematical model provides a good description of the adsorption process for Cd (II), Pb (II), and Hg (II) onto fixed bed of baker's yeast biomass.

Keywords: Biosorption; Yeast; Cd (II); Pb (II); Hg (II); Fixed bed; Mathematical model; Mass transfer coefficient

1. Introduction

The intensification of industrial activity during recent years is greatly contributing to the increase of heavy metals in the environment, mainly in the aquatic systems [1]. Wastewater contained with heavy metals is a serious environmental problem because they do not undergo biodegradation and are accumulated into the organism entering into the food chains [2]. Metals can be toxic to microbial population at sufficiently high concentrations. However, some metals are markedly more toxic even at very low levels. Among the toxic heavy metals, mercury, lead, and cadmium, "called the big three" are in the limelight due to their major impact

on the environment; Lead and cadmium are potent neurotoxic metals [3].

The sources of human exposure to Cd (II) include atmospheric, terrestrial, and aquatic routes [4]. The most severe form of Cd (II) toxicity in humans is "itai-itai", a disease characterized by excruciating pain in the bone [5]. Other health implications of Cd(II) in humans include kidney dysfunction, hepatic damage, and hypertension [6]. However, it has been suggested that overall nutritional status (rather than more Cd (II) content of food) is a more critical factor in determining Cd (II) exposure [7].

Lead (II) is heavy metal poison which forms complexes with oxo-groups in enzymes to affect virtually all steps in the process of hemoglobin synthesis and prophyrin metabolism. Toxic levels of Pb (II) in man

*Corresponding author

have been associated with encephalopathy seizures and mental retardation [8].

Mercury pollution results from metallurgical industries, chemical manufacturing, and metal finishing industries. Hg (II) in the liquid form is not dangerous and it is used in a number of industries. In the vapor form mercury becomes very poisonous. It attacks the lungs, kidneys, and the brain. The vapor crosses the blood–brain and blood stream [9].

Adsorption has been shown to be the most promising option for all these non-biodegradable heavy metals for the removal from aqueous streams, activated carbon being the most common adsorbent for this process due to its effectiveness and versatility. Although activated carbon, in granular or powdered form has a good capacity for the adsorption of heavy metals, it suffers from a number of disadvantages. Activated carbon is quite expensive and the higher the quality the greater the cost. Both chemical and thermal regeneration of spent carbon are expensive [10].

Alternatively, the so-called biosorption, i.e., the passive uptake of pollutants from aqueous solutions by the use of non-growing or non-living microbial mass, thus allowing the recovery and/or environmentally acceptable disposal of the pollutants, could also be considered. “Biosorption” term is used to indicate a number of metabolism-independent processes (physical and chemical adsorption, electrostatic interaction, ion exchange, complexation, chelation, and microprecipitation) taking place essentially in the cell wall rather than oxidation through anaerobic or aerobic metabolism (biodegradation). The main attractions of biosorption are high selectivity and efficiency, cost effectiveness and good removal performance [11].

The use of dead microbial cells in biosorption is more advantageous for water treatment in that dead organisms are not affected by toxic wastes, they do not require a continuous supply of nutrients and they can be regenerated and reused for many cycles. Dead cells may be stored or used for extended periods at room temperature without putrefaction occurring. Moreover, dead cells have been shown to accumulate pollutants to the same or greater extent than growing or resting cells.

However, the use of dead biomass in powdered form in the column has some problems, such as difficulty in the separation of biomass after biosorption, mass loss after regeneration, low strength and density and small particle size, which makes it difficult to use in column applications. To solve these problems, dead biomass can be immobilized in a supporting material [12].

Yeast biomass plays an important role in investigations in the field of biosorption. Yeast is an inexpensive, easily available source of biomass. Yeast cells

are known to bind various metal ions from solution under a wide range of external conditions [13]. Continuous packed bed column systems are the most suitable and economic ways to remove heavy metals, offering an alternative treatment for the removal and recovery of heavy metals in aqueous systems. Breakthrough curves are necessary for the adsorption column design, due to the information about the dynamic behavior of the metal concentration of the effluent in time. Another important factor for the column design is the maximum capability of adsorption of the metallic ion with a specific amount of biomass; this process is studied with the help of sorption isotherms. Mathematical models were carried out for the adjustment of experimental breakthrough curves, and the dynamic behavior prediction of the column in biosorption processes. These models are useful for the sizing and optimization of the industrial scale process using laboratory data; mathematical models also enable the response and mechanisms prediction of the system [14].

The aim of the present research is to investigate the lead, cadmium, and mercury ions (single, binary, and ternary) biosorption batch processes using baker’s yeast as a biosorbent, as well as the effect of different influent adsorbates concentration, and flow rate on the performance of fixed bed adsorber for the three heavy metals.

2. Mathematical models

2.1. Kinetics models

There are various kinetic models have been used for evaluating the intraparticle diffusion coefficients. The pseudo-first-order rate expression of Lagergren [13] is generally described by the following equation:

$$\frac{dq_t}{dt} = k_1(q_e - q_t) \quad (1)$$

where q_e and q_t are the amounts of each solute (mg/g) adsorbed onto the adsorbent at equilibrium and time t , respectively, k_1 is the rate constant (min^{-1}). Integrating and applying the boundary conditions, $t = 0$ and $q_t = 0$ to $t = t$ and $q_t = q_e$, Eq. (1) takes the form:

$$\ln(q_e - q_t) = \ln q_e - k_1 t \quad (2)$$

While the linearized form of the pseudo-second-order equation [15] is given by:

$$\frac{t}{q_t} = \frac{1}{k_2 q_e^2} + \frac{1}{q_e} t \quad (3)$$

where k_2 is the rate constant of pseudo-second-order biosorption ($\text{mg g}^{-1} \text{min}^{-1}$); q_e is the amount of metal adsorbed at equilibrium (mg g^{-1}); and q_t is the amount of metal adsorbed at time t (mg g^{-1}).

Replacing the initial sorption rate k_2 by h , one can get:

$$\frac{1}{q_t} = \frac{1}{h} \cdot \frac{1}{t} + \frac{1}{q_e} \quad (4)$$

2.2. Breakthrough curves model

A two parameters model for the modeling of breakthrough curves described by Belter et al. [16] takes the form:

$$\frac{C_e}{C_0} = \frac{1}{2} \left[1 + \text{erf} \left[\frac{t - t_0}{\sqrt{2\sigma t_0}} \right] \right] \quad (5)$$

where $\text{erf}(x)$ is the error function of x , t is the column residence time, t_0 is the time at which the effluent concentration is half the influent concentration, and σ represents the standard deviation which is a measure of the slope of the breakthrough curve. The model parameters t_0 and σ can be estimated by fitting Eq. (5) to experimental breakthrough data. Since major process variables such as influent flow rate, column length, and adsorbent particle size are not incorporated in Eq. (5), therefore it is necessary to empirically correlate the two model parameters with these variables in order to use Eq. (5) to simulate the dynamics of a biosorption column operated under varying experimental conditions [17].

MATLAB was used for the mathematical solution of the above equation. The breakthrough curve presented in terms of the dependence time of the relation between the final and initial Cd (II), Pb (II), and Hg (II) concentrations (C/C_0).

3. Materials and methods

3.1. Materials

Adsorbent: The yeast used in the experiments was supplied from Pakgida Company, Turkey.

Adsorbates: Cadmium, lead, and mercury ions were prepared by dissolving cadmium salt $\text{Cd}(\text{NO}_3)_2$, lead salt $\text{Pb}(\text{NO}_3)_2 \cdot 2\text{H}_2\text{O}$, and mercury salt HgCl_2 in distilled water, respectively. These solutions were kept at room temperature.

3.2. Methods

Physical properties of baker's yeast were measured at Oil Research and Development Centre, Baghdad,

Table 1
Characteristics of yeast

Bulk density (kg/m^3)	692.6
Porosity	0.36
Actual density (kg/m^3)	1406.5
Surface area (m^2/g)	2.6599

Iraq, and listed in Table 1. The non-living yeast biomass was dried in an oven at 120°C for 24 h before being used as adsorbent. The aqueous solution of cadmium, mercury, and lead were prepared from reagent grades.

For the determination of adsorption isotherms, nine 250 ml flasks were filled with known concentration of solute and a known weight of yeast. The flasks were then placed on a shaker and agitated continuously for 30 h at 30°C . The concentration of solute in the solution was determined using atomic absorption spectrophotometer (Type Perkin-Elmer -5000, USA). This experiment was carried out for single adsorbate, binary, and ternary adsorbates.

The adsorbed amount is calculated by the following equation:

$$q_e = \frac{V_L(C_0 - C_e)}{W_A} \quad (6)$$

The mass transfer coefficient for each adsorbate was estimated using the following steps:

- Estimating the optimum agitating speed for batch adsorber to reach the needed equilibrium concentration of Cd (II), Pb (II), and Hg (II).
- Estimating the mass transfer coefficient (k_2) in batch process at optimum agitation speed for each component using pseudo-second order model.

The mass transfer coefficient for Cd (II), Pb (II), and Hg (II) were obtained by using 2 L Pyrex beaker fitted with a variable speed mixer. The beaker was filled with 1 L of known concentration solution and agitation started before adding the yeast. At time zero, the accurate weight of yeast was added. Samples were taken every 5 min.

The necessary dosage of yeast to reach equilibrium related concentration of C_e/C_0 equal 0.05, were calculated by using Eq. (6).

The fixed bed adsorber experiments were carried out in a glass column of 50 mm internal diameter and 50 cm height. A 100 g of yeast was mixed with 480 g glass beads of 1 mm size (these weights were selected after many trials to fix the yeast in the bed) for each experiment in the fixed bed at

Table 2
Parameters of isotherm for Cd (II), Pb (II), and Hg (II) and correlation coefficient for various models

Model	Parameters	Cadmium	Lead	Mercury
Langmuir $q_e = \frac{q_m b C_e}{1 + b C_e}$	q_m	0.373	0.3101	0.348
	$b, m^3/kg$	13.154	205.5	116.303
	Correlation coefficient	0.9992	0.9987	0.9995
Freundlich $q_e = K C_e^{1/n}$	K	4.3453	61.422	37.24
	n	1.27	1.012	1.24
	Correlation coefficient	0.9886	0.987	0.9766
Radk-Prausnitz $q_e = \frac{K_{RP} C_e}{1 + \left(\frac{K_{RP}}{F_{RP}}\right) C_e^{1-N_{RP}}}$	K_{RP}	25.62	65.6	34.6
	F_{RP}	0.812	9.0572	5.2805
	N_{RP}	74401	-3.221	-1.58522
	Correlation coefficient	0.9736	0.97599	0.9773
Reddlich-Peterson $q_e = \frac{A_R C_e}{1 + B_R C_e^{m_R}}$	A_R	5.1617	65.536	34.688
	B_R	0.1	8.401	6.657
	m_R	5.851808	4.069189	2.577402
	Correlation coefficient	0.9879	0.9788	0.9321
Combination of Langmuir-Freundlich $q_e = \frac{b q_m C_e^{1/n}}{1 + b C_e^{1/n}}$	q_m	15.29367	138.955	201.291
	B	0.18667	1.01213	0.207137
	n	1.14616	0.482614	0.779962
	Correlation coefficient	0.9939	0.9921	0.9943

different effluent concentrations and flow rate of Cd (II), Pb (II), and Hg (II). The mixture of yeast and glass beads were confined in the fixed bed by fine stainless steel screen and two layers of fine texture at the bottom and glass packing at the top of the bed to ensure a uniform distribution of influent through the yeast bed. The influent solution was introduced to the column through a perforated plate fixed at the top of the column. Feed solution was prepared in a stainless steel vessel supplied with immersed heater and a thermocouple to adjust the temperature of the solution to 30°C.

4. Results and discussion

4.1. Adsorption isotherm

The equilibrium isotherms display a nonlinear dependence on the equilibrium concentration. The adsorption data for both systems were fitted by Langmuir model [18], Freundlich model [19], Radke-Prausnitz model [20], Reddlich-Peterson [21], and Combination of Langmuir-Freundlich isotherm model [22]. The determination coefficients are shown in Table 2 for the Cd (II), Pb (II), and Hg (II) systems. Table 2 indicates that Langmuir model provides the best fit as judged by its correlation coefficient for the three components.

The pH values for Cd (II), Pb (II), and Hg (II) were 6.22, 5.01, and 6.15, respectively, and after mixing with yeast the pH values became 4, 4.6, and 5.4, respectively.

The equilibrium isotherms for each single component Cd (II), Pb, and Hg (II) onto yeast are presented in Fig. 1, and the adsorption isotherms for each solute in the presence of other solutes are shown in Figs. 2–4. Fig. 5 represents the isotherm curve for the three solutes together, which showed the equilibrium isotherm of each solute is of favorable type. It was found that the amount of adsorbate adsorbed per unit mass of yeast for Pb (II) is greater than that for Hg (II) and Cd (II). This can be explained by the effect of solubility, where the solubility of lead nitrate salt in water is less than that of mercury chloride salt and cadmium nitrate salt. It is expected to have a highest adsorption rate.

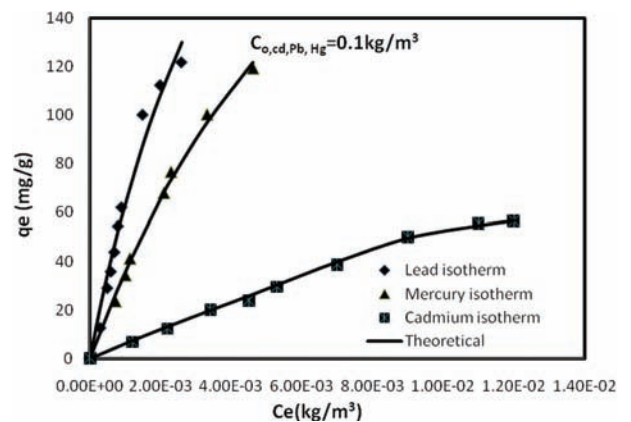


Fig. 1. Adsorption isotherm for single systems of Cd (II), Pb (II), and Hg (II) onto yeast at 303K using initial concentration for each ion 0.1 kg/m³.

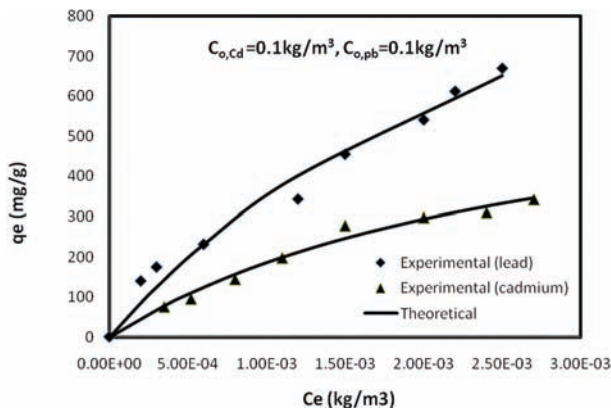


Fig. 2. Adsorption isotherm for a binary system of Cd (II) and Pb (II) onto yeast at 303 K using initial concentration for each ion 0.1 kg/m^3 .

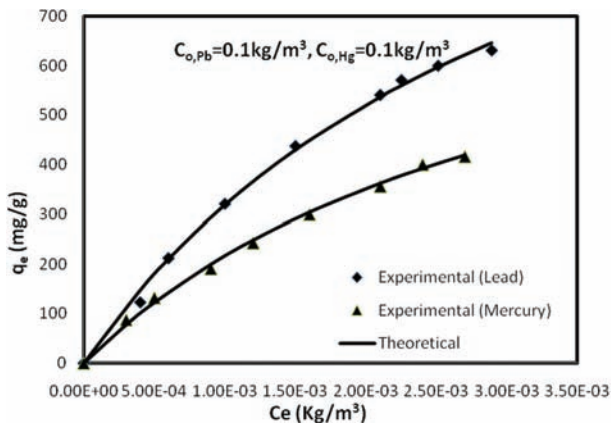


Fig. 3. Adsorption isotherm for a binary system of Pb (II) and Hg (II) onto yeast at 303 K using initial concentration for each ion of 0.1 kg/m^3 .

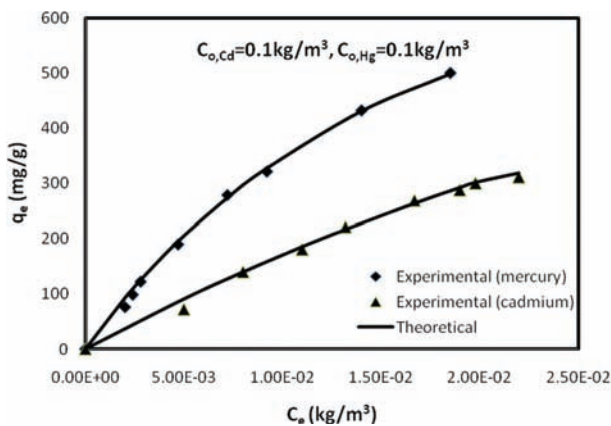


Fig. 4. Adsorption isotherm for binary system of Cd (II) and Hg (II) onto yeast at 303 K using initial concentration for each ion 0.1 kg/m^3 .

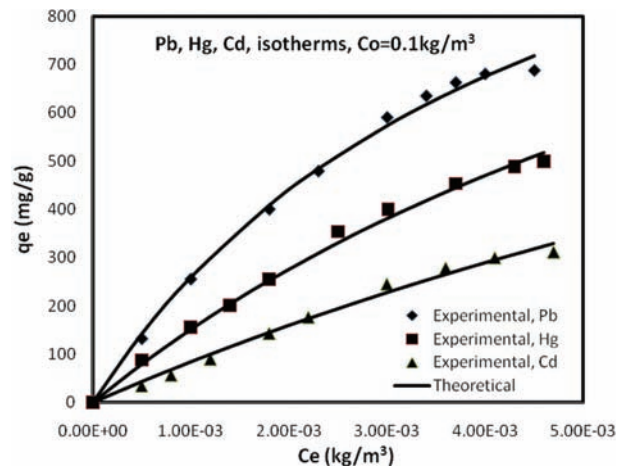
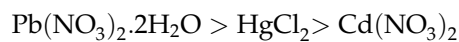


Fig. 5. Adsorption isotherm for ternary system of Pb (II), Cd (II), and Hg (II) onto yeast at 303K using initial concentration for each ion 0.1 kg/m^3 .

Furthermore it may be related to the molecular weight, where the higher adsorption rate related to the higher molecular weight salt.



4.2. Mass transfer coefficient

The amounts of yeast used for adsorption of Cd (II), Pb (II), and Hg (II) were calculated for final equilibrium related concentration of $C_e/C_0 = 0.05$. The initial concentrations for each solute was 0.1 kg/m^3 with the doses of yeast for Cd (II), Pb (II), and Hg (II) systems are $3.4 \times 10^{-3} \text{ kg}$, $0.5 \times 10^{-3} \text{ kg}$, and $0.75 \times 10^{-3} \text{ kg}$, respectively.

The typical concentration decay curves of solute in batch experiments were carried out for Cd (II), Pb (II), and Hg (II) at different agitation speeds as shown in Figs. 6, 7, and 8, respectively. The optimum agitation speed needed to achieve $C_e/C_0 = 0.05$ was found to be 1,000 rpm.

The adsorption data at optimum agitation speed for the three solutes were analyzed in terms of pseudo-first and second-order mechanisms.

The rate constant using pseudo-first-order rate expression was obtained from the slope of the linear plots of $\log(q_e - q_t)$ against t for each solute using Eq. (2). While, the rate constants for Cd (II), Pb (II), and Hg (II) by using pseudo-second-order biosorption rate constant (k_2) were determined from the slope and intercept of the plots of $1/q_t$ against $1/t$ using Eq. (4). The values of the rate constants with the corresponding correlation coefficients are presented in Table 3 for both kinetic models and for the three solutes

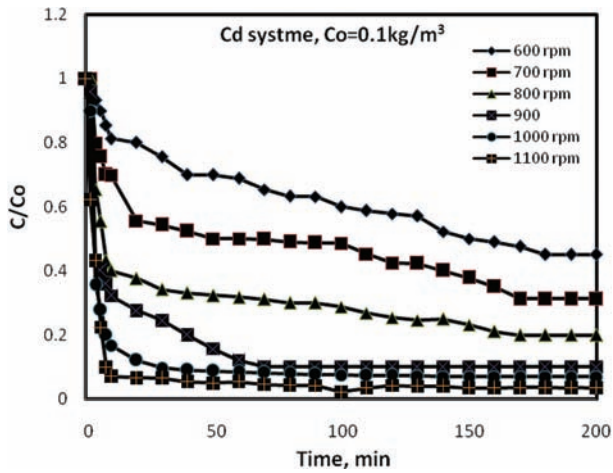


Fig. 6. Concentration-time decay curves for Cd (II) adsorption onto yeast at different agitation speed using initial concentration 0.1 kg/m^3 .

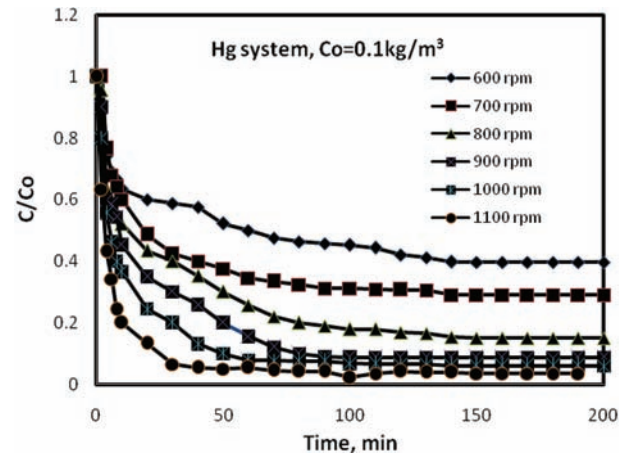


Fig. 8. Concentration-time decay curves for Hg (II) adsorption onto yeast at different agitation speed using initial concentration 0.1 kg/m^3 .

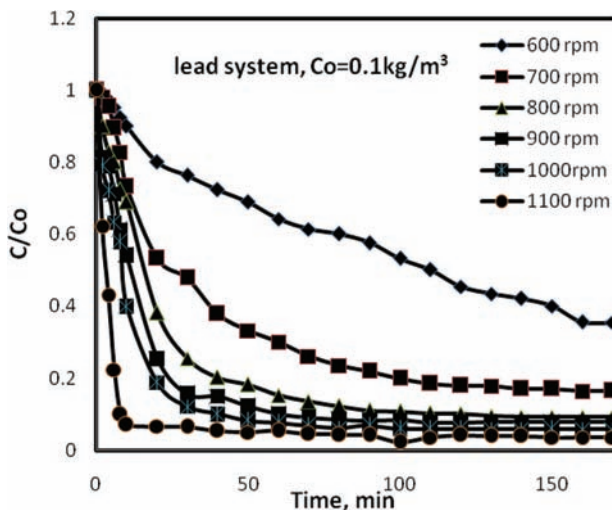


Fig. 7. Concentration-time decay curves for Pb (II) adsorption onto yeast at different agitation speed using initial concentration 0.1 kg/m^3 .

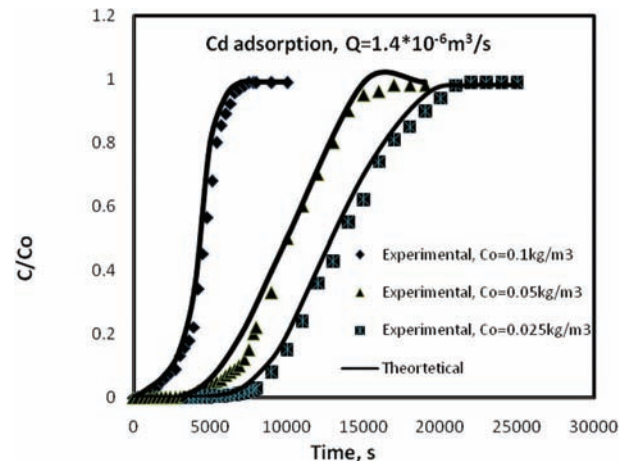


Fig. 9. Experimental and theoretical breakthrough curves for adsorption of Cd (II) onto yeast at different initial concentrations and $Q = 1.4 \times 10^{-6} \text{ m}^3/\text{s}$.

Table 3
Pseudo first and second order rate constants for Cd (II), Pb (II), and Hg (II) with correlation coefficients

Pollutant	Pseudo-first order kinetic model		Pseudo-second order kinetic model	
	K_1 (min^{-1})	R^2 (correlation coefficient)	K_2 (mg/g min)	R^2 (correlation coefficient)
Cd (II)	0.002	0.516	6.099×10^{-4}	0.963
Pb (II)	0.016	0.856	1.259×10^{-3}	0.979
Hg (II)	0.005	0.804	9.6×10^{-4}	0.960

As can be seen from Table 3, the correlation coefficients for the pseudo-first-order kinetic model for the various solutes were found to be lower than that for the pseudo-second-order kinetic. Therefore, the pseudo-second-order kinetics model can be used very well to find the rate constant. From Table 3, Pb (II) has the largest value of pseudo-second and first-order rate constants in comparison with Hg (II) and Cd (II). This enhances the results regarding Pb (II) for its fastest adsorption onto yeast.

4.3. Breakthrough curves for packed bed adsorber

4.3.1. Effect of influent concentrations

Figs. 9, 10, and 11 show the experimental and predicted breakthrough curves for Cd (II), Pb (II), and

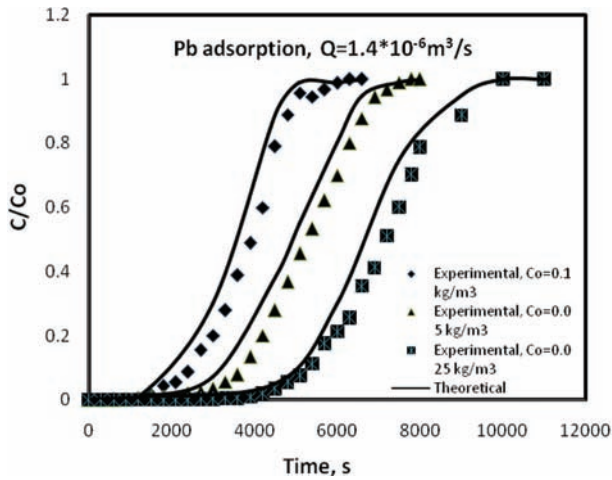


Fig. 10. Experimental and theoretical breakthrough curves for adsorption of Pb (II) onto yeast at different initial concentrations and $Q=1.4 \cdot 10^{-6} \text{ m}^3/\text{s}$.

Hg (II), respectively, for adsorption onto baker's yeast at different initial concentrations of adsorbate at constant temperature of 303 K. It can be seen that an increase in the initial concentration of Cd (II), Pb (II), and Hg (II) make the breakthrough curves much steeper, this would be anticipated on the basis that the driving force for mass transfer increases with increase of concentration of adsorbates in the solution [23]. A high adsorbates concentration may saturate the adsorbent more quickly, thereby decreasing the breakthrough time. The same conclusion was obtained by Ref. [24,25]. There is a good matching between the predicted and the experimental breakthrough curves, as shown in the figures.

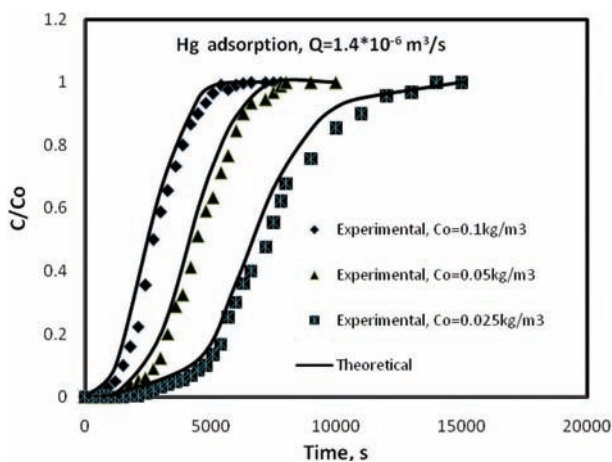


Fig. 11. Experimental and theoretical breakthrough curves for adsorption of Hg (II) onto yeast at different initial concentrations and $Q = 1.4 \cdot 10^{-6} \text{ m}^3/\text{s}$.

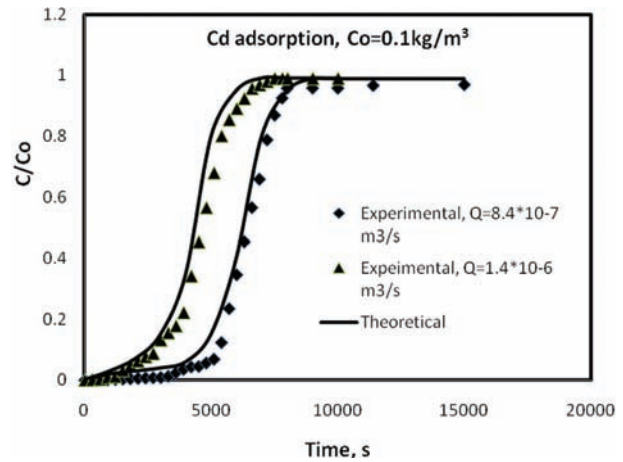


Fig. 12. Experimental and theoretical breakthrough curves for adsorption of Cd (II) onto yeast at different flow rates and $C_o = 0.1 \text{ kg/m}^3$.

4.3.2. Effect of flow rates

Figs. 12, 13, and 14 present the experimental and predicted breakthrough curves for Cd (II), Pb (II), and Hg (II), respectively, for adsorption onto baker's yeast at different flow rates of adsorbate at constant temperature of 303 K. An increase in the adsorbate flow rate decreases the breakthrough time due to the decrease in the contact time between the adsorbate and the adsorbent along the adsorption bed. Increasing the flow rate may be expected to make reduction of the liquid film thickness. Therefore, this will decrease the resistance to mass transfer and increase the mass transfer rate as well as there is not enough time for adsorption equilibrium to be reached. These phenomena agree with that obtained by Ref. [26,27].

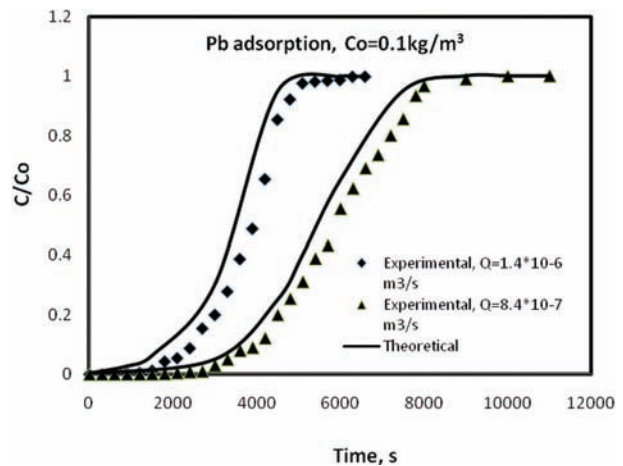


Fig. 13. Experimental and theoretical breakthrough curves for adsorption of Pb (II) onto yeast at different flow rates and $C_o = 0.1 \text{ kg/m}^3$.

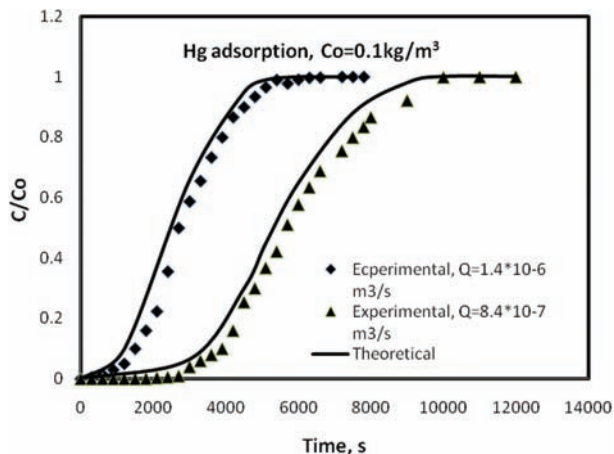


Fig. 14. Experimental and theoretical breakthrough curves for adsorption of Hg (II) onto yeast at different flow rates and $C_0 = 0.1 \text{ kg/m}^3$.

5. Conclusions

The equilibrium isotherm data were correlated with five models for each solute, Langmuir model gave the best fit for the experimental data for all of them. The batch experiments were helpful in estimating the optimum agitating speed for each solute and to find the rate constants for Cd (II), Pb (II), and Hg (II) by using pseudo-first and second-order models, the results showed that the Cd (II), Pb (II), and Hg (II) uptake process followed the pseudo-second-order rate model. A two parameters model for the modeling of breakthrough curves was used. An increase in the initial concentration of each adsorbate makes the breakthrough curves much steeper, which would be anticipated with the basis of increases driving force for mass transfer with the increase of adsorbates concentrations. The increase in the flow rate for each solute decreases the breakthrough time due to the decrease in the contact time between the adsorbate and the adsorbent along the adsorption bed.

Acknowledgment

We would like to express our sincere thanks and deep gratitude to the Ministry of Higher Education and Scientific Research, Research and Promotion Office for supporting this work financially.

Symbols

A_R	Reddlich-Peterson model parameter
B	Langmuir constant, l/mg
B_R	Reddlich-Peterson model parameter
C	Concentration of fluid, kg/m^3
C_0	Initial concentration, kg/m^3

C_e	Concentration of solute at equilibrium, kg/m^3
F_{RP}	Radke-Prausnitz model parameter
Q	Flow rate, m^3/s
K	Freundlich empirical constant
K_{RP}	Radke-Prausnitz model parameter
m_R	Reddlich-Peterson model parameter
N_{RP}	Radke-Prausnitz model parameter
n	Freundlich empirical constant
V_L	Volume of solution, m^3
W_A	Mass of adsorbent, kg

References

- [1] P.A. Marques, M.F. Rosa and H.M. Pinheiro, PH effects on the removal of Cu_2 , Cd_2 and Pb_2 from aqueous solution by waste brewery waste, *Bioprocess Eng.*, 23 (2000) 135–141.
- [2] C. Cojocarua, M. Diaconua, I. Cretescua, J. Savi and V. Vasi, Biosorption of copper ions from aqua solutions using dried yeast biomass, *Coll. Surf. A: Physicochem. Eng. Asp.*, 335 (2009) 181–188.
- [3] P.R. Puranik and K.M. Paknikar, Biosorption of lead and zinc from solution using streptovorticillium waste biomass, *J. Biotechnol.*, 55 (1997) 113–124.
- [4] K.A. Wolnik, F.L. Frick, S.G. Caper, M.W. Meyer and R.D. Sattergar, Cadmium lead and eleven other elements in carrots field corn, onion, rice, spinach and tomatoes, *J. Agric. Food Chem.*, 33 (1985) 807–811.
- [5] M. Yasuda, A. Miwa and M. Kitagawa, Morphometric studies of renal lesions in "Itai-itai" disease: chronic cadmium nephropathy, *Nephron*, 69 (1995) 14–19.
- [6] C.D. Klaassen, J.G. Hardmen, L.E. Limbird and A.G. Gilman, *The Pharmacological Basis of Therapeutics*, McGraw Hill, New York, 2001.
- [7] M. Vahter, M. Berghund, B. Nermell and A. Akesson, Bioavailability of cadmium from shell fish and mixed diet in women, *Toxicol. Appl. Pharmacol.*, 136 (1996) 332–334.
- [8] C.M.A. Ademorati, *Environmental Chemistry and Toxicology. Pollution by Heavy metals*. Fludex press Ibadan (1996) 171–172.
- [9] J.C. Igwe and A.A. Abia, A bioseparation process for removing heavy metals from wastewater using biosorbents, *Afric. J. Biotechnol.* 5 (12) (2006) 1167–1179.
- [10] Y. Fu and T.F. Viraraghavan, Decolourization of wastewaters: a review, *Bioresour. Technol.*, 79 (2001) 251–262.
- [11] T. O'Mahony, E. Guibal and J.M. Tobin, Reactive dye biosorption by *Rhizopus arrhizus* biomass. *Enzyme Microbial Technol.*, 31 (2002) 456–463.
- [12] A. Zümriye, Application of biosorption for the removal of organic pollutants: a review, *Process Biochem.*, 40 (2005) 997–1026.
- [13] V. Padmavathy, Biosorption of nickel(II) ions by baker's yeast: Kinetic, thermodynamic and desorption studies, *Bioresour. Technol.*, 99 (2008) 3100–3109.
- [14] C.M. Ramirez, M. Pereira da Silva, G. Selma, L. Ferreira and E. Oscar Vasco, Mathematical models applied to the Cr(III) and Cr(VI) breakthrough curves, *J. Hazard. Mater.*, 146 (2007) 86–90.
- [15] P. Vasudevan, V. Padmavathy and S.C. Dhingra, Kinetics of biosorption of cadmium on Baker's yeast, *Bioresour. Technol.*, 89 (2003) 281–287.
- [16] P.A. Belter, E.L. Cussler and W.S. Hu, *Bioseparations, Downstream Processing for Biotechnology*, John Wiley & Sons, New York, 1988.
- [17] J.M. Brady, J.M. Tobin and J.C. Roux, Continuous fixed bed biosorption of Cu_2 . Ions: application of a simple two parameter mathematical model, *J. Chem. Technol. Biotechnol.*, 74 (1999) 71–77.

- [18] S. Lucas and M.J. Cocero, Adsorption isotherms for ethylacetate and furfural on activated carbon from supercritical carbon dioxide, *Fluid Phase Equilib.*, 219 (2004) 171–179.
- [19] J.R. Weber and J. Walter, *Physicochemical Processes for Water Quality Control*, Wiley Inter Science, New York, 1972.
- [20] C.J. Radke and J.M. Prausnitz, Adsorption of organic compounds from dilute aqueous solution on activated carbon, *Ind. Eng. Chem. Funda.*, 11 (1972) 445–451.
- [21] L. Jossens, J.M. Prausnitz and W. Frits, Thermodynamic of multi-solute adsorption from dilute aqueous solutions, *Chem. Eng. Sci.*, 33 (1978) 1097–1106.
- [22] R. Sips, *J. Chem. Phys.*, 16 (1984) 490–495.
- [23] E. Malkoc and Y. Nuhoglu, Fixed bed studies for the sorption of chromium (VI) onto tea factory waste, *Chem. Eng. Sci.*, 61 (2006) 4363–4372.
- [24] A.H. Sulaymon and K.W. Ahmed, Competitive adsorption of furfural and phenolic compounds onto activated carbon in fixed bed column, *Environ. Sci. Technol.*, 42 (2007) 392–397.
- [25] A.H. Sulaymon, A.M. Ali and S. Al-Naseri, Natural organic matter removal from Tigris River water in Baghdad, Iraq, *Desalination*, 245 (2009) 155–168.
- [26] A.H. Sulaymon, A. Balasim, Abid and J.A. Al-Najar, Removal of lead, copper, chromium and cobalt ions onto granular activated carbon in batch and fixed bed adsorbers, *Chem. Eng. J.*, 155 (2009) 647–653.
- [27] A.H. Sulaymon and Sh.E. Ebrahim, Saving amberlite XAD4 by using inert material in adsorption process, *Desalination Water Treat. J.*, 20 (2010) 234–242.